

11. Shen, Z. and He, Z., Interaction between *eui* gene and WAMS cytoplasm of rice and improvement of panicle exertion of MS line. In Proc. SABRAO Congr. Tsukuba, Japan, 21–25 August 1989, pp. 753–756.
12. He, Z. and Shen, Z., Inheritance of panicle exertion and improvement of male sterile line in rice (In Chinese with English summary). *Chin. J. Rice Sci.*, 1991, **5**, 1–6.
13. Virmani, S. S., Dalmacio, R. D. and Lopez, M. T., *eui* gene for elongated uppermost internode transferred to indica rice. *Int. Rice Res. Newsl.*, 1988, **13**, 6.
14. Mackill, D. J., Rutger, J. N. and Johnson, C. W., Elongated uppermost internode (*eui*) is a recurring mutation. *Rice Genet. Newsl.*, 1992, **9**, 102–103.
15. Yang, R. C., Yang, S. L., Zhang, Q. Q., and Huang, R. H., A new elongated uppermost internode gene. *Rice Genet. Newsl.*, 1999, **16**, 41–43.
16. Yang, R. C., Zhang, S., Huang, R., Yang, S. and Zhang, Q., Breeding technology of *eui*-hybrids of rice. *Agric. Sci. Chin.*, 2002, **1**, 59–363.
17. Zhou, G., Li, X. and Zhou, J., Breeding and using thermosensitive genic male sterile rice with elongated uppermost internode. Proc. 4th Int. Symp. Hybrid Rice, Hanoi, Vietnam, IRRI, Manila, Philippines, 14–17 May 2002.
18. Zhang, S., Huang, R., Zhang, Q., Wang, N. and Yang, R. C., Development of the TGMS line Peiai 64es1 with the *eui* gene. Proc. 4th Int. Symp. Hybrid Rice, Hanoi, Vietnam, IRRI, Manila, Philippines, 14–17 May 2002.
19. Librojo, A. L. and Khush, G. S., Chromosomal location of some mutant genes through the use of primary trisomics in rice. In *Rice Genetics*, IRRI, Manila, Philippines, 1986, pp. 249–255.
20. Wu, Y. *et al.*, The RFLP of tagging of *eui* gene in rice (In Chinese with English summary). *Chin. J. Rice Sci.*, 1998, **12**, 119–120.
21. Yang, S. L., Ma, H. L., Xue, Q. P., Wang, B. and Yang, R. C., Tagging of an elongated-uppermost internode gene *eui2* using microsatellite markers. *Rice Genet. Newsl.*, 2000, **17**, 1–2.
22. Dellaporta, S. L., Wood, J. and Hicks, J. B., A plant DNA mini-preparation: Version II. *Plant Mol. Biol. Rep.*, 1983, **1**, 19–22.
23. Gomez, K. A. and Gomez, A. A., *Statistical Procedures for Agricultural Research*, John Wiley, New York, 1984, 2nd edn.
24. Strickberger, M. W., *Genetics*, Macmillan, New York, 1977, 2nd edn.

ACKNOWLEDGEMENTS. We thank Dr Gurdev S. Khush, IRRI, Manila, Philippines for providing seeds of IR91-1591-3; Dr Usha B. Zehr, Director and Dr George Thottappilly, Executive Director, MAHYCO Research Foundation, Hyderabad, for support and encouragement.

Received 27 January 2004; revised accepted 3 April 2004

A study of rainfall along the west coast of India in relation to low level jet and air–sea interactions over the Arabian Sea

A. K. Mishra, C. Gnanaseelan* and P. Seetaramayya

Indian Institute of Tropical Meteorology, Pune 411 008, India

Indian summer monsoon has a large inter-annual as well as intra-seasonal variability over temporal and spatial scales. Onset dates, monsoon activity within a monsoon season and quantity of monsoon rainfall are also found to vary from year to year. One important synoptic feature associated with the onset of monsoon is the existence of a strong cross equatorial low level jet (LLJ), with its core around 850 hPa over the Indian Ocean and South Asia. This LLJ generally supports the large-scale moisture and momentum transport from ocean to atmosphere and the consequent rainfall over the Indian mainland. In the present study, buoy data at a stationary position in the Arabian Sea (15.5°N, 61.5°E) have been used to understand the air–sea interface processes before, during and after the onset of monsoon 1995.

A remarkable feature of the summer monsoon over the Indian Ocean (IO) is the gradual formation of a low-level

jet (LLJ)¹ over the western IO. Bunker² first reported the presence of LLJ off Somalia during the International Indian Ocean Expedition (IIOE, during 1962–66) in a preliminary analysis. Joseph and Raman³ have further found the existence of similar LLJs with a core speed of 20–30 m/s near 1.5 km asl over peninsular India, on several days during July. Later studies by Findlater⁴ have explained the importance of LLJ in the monsoonal activity over the Indian subcontinent. Findlater⁴ and Krishnamurti⁵ have studied the mean monthly air flow at low-levels (1.0–1.5 km) over western IO and found that the Kenyan highlands appear to be a western boundary for this major low-level air current, which is known to have a maximum mean wind speed (19 m/s) near 1.5 km level. In February, a clockwise gyre of air can be seen 10° south of the equator. Its month-by-month northward progress⁵ appears to continue until June. Thereafter, its position is relatively steady in the belt of 10–20°N until September. After September, with the cessation of the SW monsoon, the LLJ proceeds back southwestwards to the southern IO. The major axis of the jet passes through the points

*For correspondence. (e-mail: seelan@tropmet.res.in)

20°S, 60°E; 12°S, 48°E; 0°N, 40°E; 5°N, 42°E; 10°N, 50°E. At 12°N, 58°E the jet splits into two, the northward branch of major axis passes through 15°N, 60°E; 17°N, 72°E and Indian mainland. The southward branch (secondary axis) of the split moves southeastward, just south of India. Krishnamurti⁵ has further revealed that the west coast of India near 17°N gets copious rainfall when the northern branch of the jet is strong and active during the monsoon months. Stommel and Fieux⁶ have also examined the structure of the surface winds during the onset of the SW monsoon in the Arabian Sea (AS) using historical meteorological ship reports available between the equator and 20°N, and between Africa and India (Marsden squares; 29, 30, 31, 32, 66, and 67, vide their Figure 1) for the period between 1900 and 1973. They have tried to detect a link between the onset of the monsoon near the Somali coast and rainfall over the Indian peninsula. Stommel and Fieux have also shown similar axes of surface air current over the central AS, whereby both the axes coincide with the Findlater jet axes at 850 hPa east of 60°E. But a split in the Findlater jet takes place near the 12°N, 58°E, while the split in the Stommel and Fieux⁶ axis takes place near the African coast (10°N). Further, Stommel and Fieux correlated the mean June rainfall data in the west coast of India with the onset near Somali coast in May. They found high correlation coefficient (CC) between the date of onset near the Somali coast (10–12°N, 51–53°E) and mean rainfall in June over Konkan (Mumbai) and the onset between 10–12°N, 53–60°E and the mean rainfall in June over Kerala and coastal Mysore. The CCs were respectively, –0.54 and –0.66 (for the period 1919–39 and 1947–55) giving a significance level of 99% for Konkan and 99.9% for Kerala and coastal Mysore. Nevertheless, they emphasized that the SW monsoon winds can blow near the Arabian coast between 17 and 20°N, at the beginning of March, it perhaps cannot be called SW monsoon, but for our case it cannot be ignored. Most of the study by Stommel and Fieux⁶ is primarily based on data available in a strip (2°×2° lat by long) along African–Arabian coastline and along 10°N from Africa to India. However, data along the jet line in the central AS (15–20°N, 60–70°E) are rather meagre. Stommel and Fieux have suggested that some efforts are to be made to study the areas of the Indian peninsula in detail and to include the variation due to sea surface temperature (SST) anomalies over this part of the central AS. It is clear from previous studies that LLJ is a special synoptic feature existing during the monsoon season.

Recently, Swapna and Ramesh Kumar⁷ have examined the role of low-level flow jet on monsoon activity using 850 hPa winds for the monsoon period June–September for the years 1987 and 1988. The former is a bad monsoon year, while the latter is a good monsoon year. Their analysis has revealed that winds are high over the AS compared to central Bay of Bengal (BOB) and southern IO. The western AS has shown great contrast, where

wind speeds are about 2 m/s higher in 1988 than in 1987. They have further found that during the active monsoon periods, the core of the jet is directed to the Indian subcontinent, producing heavy rainfall over India. But during the weak periods, the core of the jet is directed south of the Indian peninsula leading to weak monsoon conditions over India. Vinayachandran *et al.*⁸ and Sijikumar *et al.*⁹ have also reported similar features in their studies. In another study, Ramesh Kumar *et al.*¹⁰ have reported a case study on the role of the cross-equatorial flow on summer monsoon rainfall over India using NCEP/NCAR reanalysis data.

Ramesh Kumar *et al.*¹⁰ have also examined an annual cycle of the moisture fluxes across different boundaries of the AS (0° to 25°N, 45 to 75°E) for the period 1982 to 1994. This study revealed that the major contribution of moisture for the AS is from the south IO and a substantial amount also comes from the western boundary, i.e. across the east coast of Africa. They have further stated that the moisture fluxes are able to depict the enhancement of moisture over the AS from April to June. The values are thus saturated and remain constant till July. From August, the cross equatorial flow decreases. The maximum contribution for the AS box from the western boundary is seen in July and August. The maximum loss from this box is to the Indian subcontinent and it increases almost two to three times from April to May/June, indicating evolution of the summer monsoon over India. Further they have mentioned that there exists a sharp rise in the moisture flux in the AS and this rise could be due to the cloudiness effect of sudden increase in the zonal component of the low-level winds as well as the increase in moisture over the AS.

However, in the present study we have examined comprehensive year-long-time series surface meteorological data of wind, air, temperature and SST, relative humidity, mean sea-level pressure from a surface mooring buoy deployed off the coast of Oman (15.5°N, 61.5°E along the climatological axis of the Findlater jet from 16 October 1994 to 19 October 1995). Weller *et al.*¹¹ have summarized the details of data collection, error analysis and some of the salient features that emerged out of the above dataset. However, in the present study we reanalyse the data by analysing the various fluxes and try to understand the plausible mechanisms for the evolution of the air–sea interface processes on timescales of a day, synoptic, intra-seasonal and seasonal basis. Further, we have also examined air–sea interface flux-transfer processes in relation to the evolution of the LLJ over the AS and the influence of LLJ on the west coast rainfall.

Data and methodology

The following data over the period of 1 May 1995 to 30 September 1995 have been consulted for the present study. They are: (i) The daily rainfall data collected at some

well-known meteorological stations (Figure 1), namely Dahanu, Mumbai, Harnai, Ratnagiri, Panjim, Karwar and Mangalore along the west coast of India ($12\text{--}20^\circ\text{N}$)¹²; (ii) Daily 850 hPa wind fields over the IO¹³ between latitudes 20°S to 25°N , and longitudes 35 and 115°E ; (iii) The surface meteorological observations taken from a stationary mooring buoy deployed off the Oman coast at 15.5°N , 61.5°E , which lies along the Findlater jet (LLJ)^{11,14,15}.

In order to find out the daily geographical position of the LLJ core at 850 hPa level over the IO region, synoptic weather charts using the daily NCEP/NCAR reanalysis data have been consulted. Figure 2 shows these charts for selected days on which the monsoon exhibits peculiar behaviour like onset, active phase, splitting of jet and break monsoon conditions. Further, in order to understand the plausible influence of LLJ on the west coast rainfall, area daily averages of zonal wind (AZW) and total column precipitable water¹³ (TCPW) for the domain $45\text{--}80^\circ\text{E}$ and $10\text{--}20^\circ\text{N}$ have been computed and plotted along with the daily surface parameters observed at WHOI buoy (Figure 3) and daily rainfall at west coast stations (Figure 4) respectively, for comparison. Weller *et al.*¹¹ provided various heat, momentum and radiational fluxes at the WHOI point. The air–sea fluxes at WHOI were computed using version 2.5 of the bulk formulae developed during COARE, described by Fairall *et al.*¹⁶. Shallowest (0.17 m) temperature observations were extrapolated to the surface to obtain a skin temperature, which is then used for flux computation. Net short-wave radiation was computed¹⁷ from incoming short-wave radiation using a variable albedo based on the solar elevation angle and an atmos-

pheric transmittance of 0.720. Net long-wave radiation was computed by subtracting an estimate of the outgoing long-wave,

$$LW\uparrow = \epsilon sT^4 + (1 - \epsilon)LW\downarrow, \quad (1)$$

where $LW\uparrow$ is the outgoing long-wave radiation, $LW\downarrow$ is the incoming long-wave radiation, emissivity $\epsilon = 0.97$ and Stefan–Boltzmann constant $s = 5.67 \times 10^{-8} \text{ W m}^{-2} \text{ K}^{-4}$.

Results

Figure 1 shows the location map of the study area. The geographical position of the stations considered as representative of the west coast and the stationary position (15.5°N , 61.5°E) of the mooring deployed off the Oman coast are shown. It is clear that all the coastal stations are between 12 and 20°N , which is the area where Findlater jet is most active during the season. To visualize the strength and location of the LLJ over the IO and its neighbourhood, we have plotted the streamlines and isotachs of the wind field over those regions where the jet core is prominent at 850 hPa level. It is well known that the LLJ originates in the southern IO, crosses the equator near Nairobi (South Africa) and turns east in the AS heading towards India during the height of the monsoon. The representative NCEP mean daily 850 hPa circulation charts from 1 May to 30 September 1995 (153 charts) have been examined carefully and charts were chosen corresponding to those dates which are relevant to the following four phases of the monsoon during the year 1995. They are: (i) Onset phase of monsoon (Figure 2a–c), (ii) active phase of monsoon (Figure 2d–f), (iii) splitting of the jet (or weak monsoon phase, Figure 2g–i) and (iv) the break phase of monsoon (Figure 2j–l). These four categories of charts were then qualitatively compared with the time series rainfall distribution at the stations along the west coast of India (Figure 1). It has been observed that rainfall along the west coast appears to have occurred during those periods where the LLJ touches the west coast. When the jet is far away or splitting and turning to the south of the trough, the west coast receives either less or no rainfall.

The onset of the SW monsoon is generally marked by a change in the wind field (180° out of phase from low to high speed) from winter to summer circulation. In South Asia, particularly over the Indian subcontinent, these are the two major circulations with contrasting features, which prevail about 4 to 6 months. A transition from winter to summer circulation is associated with some comparable changes in several meteorological parameters at the surface and in the upper air, which build-up progressively with the advance of the season and reach a critical stage by the end of May leading to the burst of monsoon. Having examined the above features carefully for many years during the period from 1901 to 1982, Ananthakrishnan *et al.*¹⁸

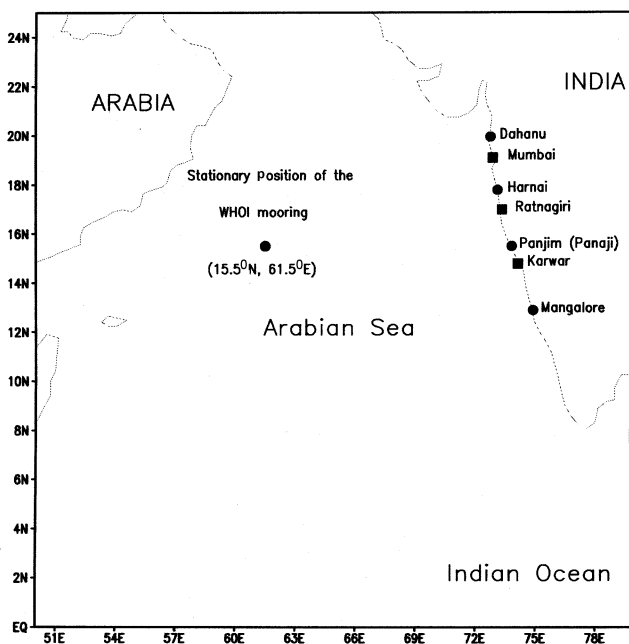


Figure 1. Location map.

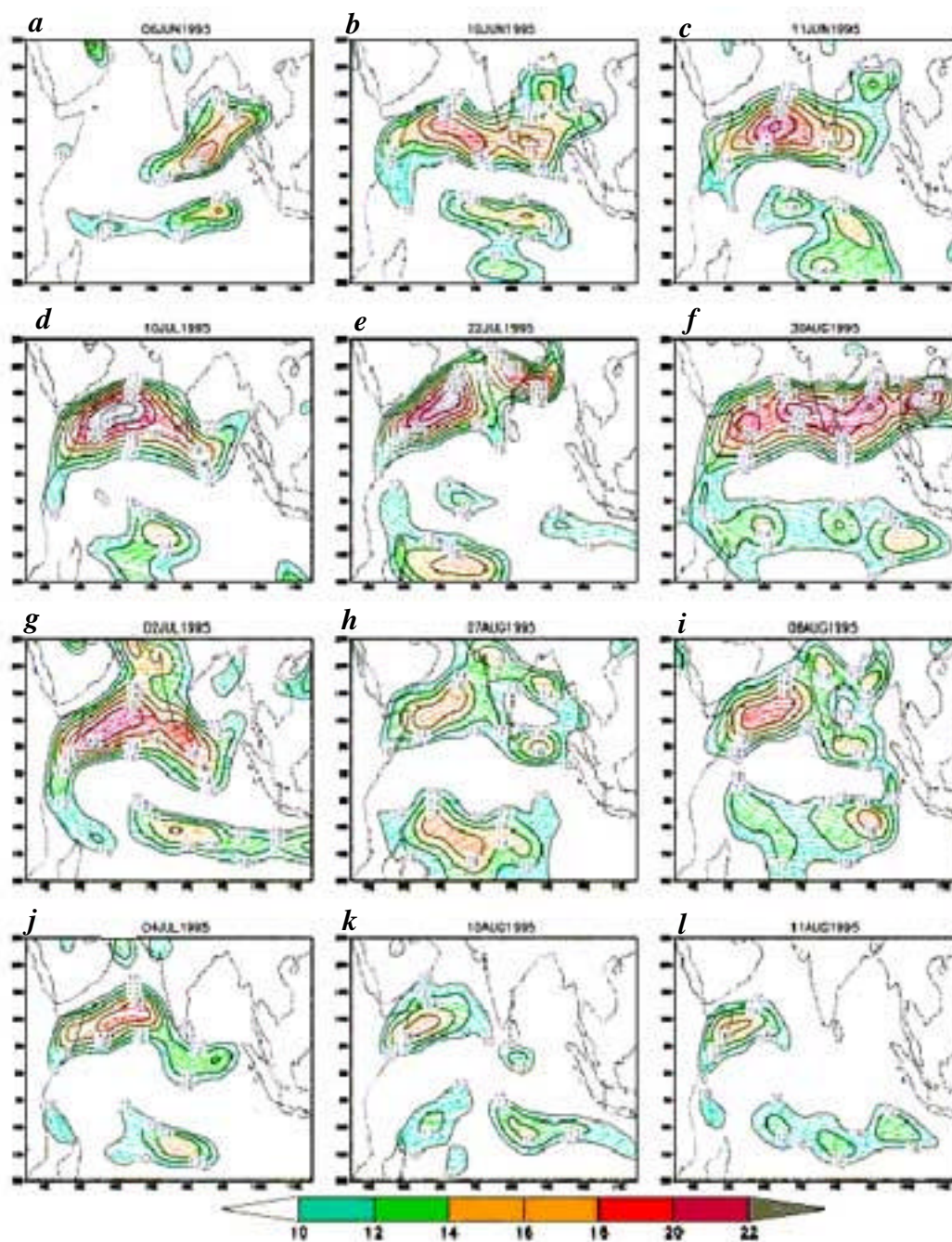


Figure 2. Low level jet (in m/s at 850 hPa) core over the north Indian Ocean during onset (plot *a-c*), active phase (*d-f*), splitting of jet (*g-i*) and break monsoon (*j-l*).

have found the normal date of onset of monsoon over the southwestern tip of India (south Kerala coast) as 1 June (i.e. the outbreak of the SW monsoon rains of at least 10 mm average rainfall in pentad (five days)¹⁹). A 'break' or 'weak' in the monsoon occurs when the normal monsoon trough over the Gangetic plains shifts northward to the foot-hills of the Himalaya. This is a short break in the prolonged monsoon activity, for a period of 2 to 5 days, during which the west coast and central part of India receive

very little or no rainfall. The revival takes place when a low-pressure system of moderate intensity forms over the head BOB²⁰.

During 1995, the onset of monsoon was delayed by about ten days from its normal date (1 June). The LLJ had not organized completely but two broken jet cores, one on either side of the equator in both hemispheres along the same longitude (85–90°E), were seen in the chart (Figure 2*a*) on 6 June. The north jet core is quite promi-

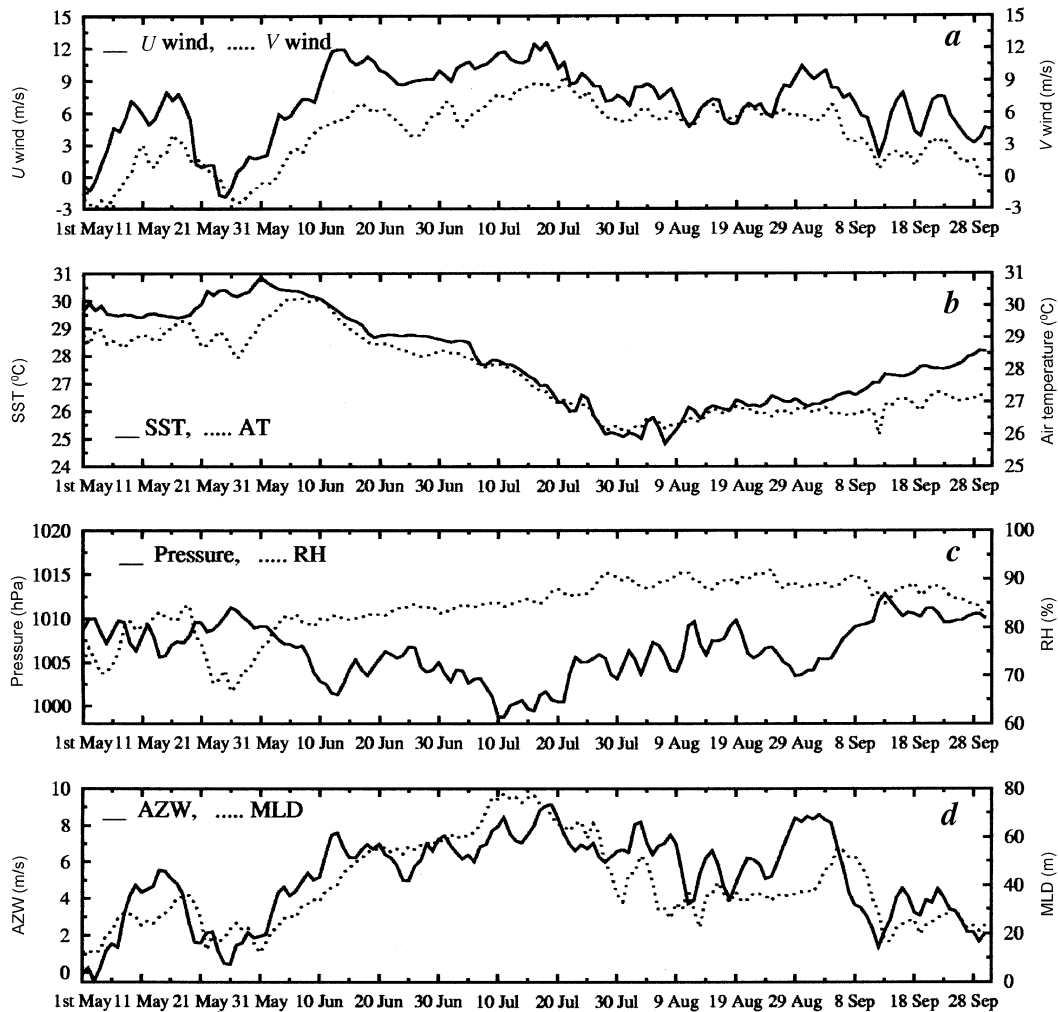


Figure 3. *a-d*, Time series of meteorological and mixed layer depth (MLD) at WHOI buoy (15.5°N , 61.5°E) and average zonal wind (AZW) over the area ($45\text{--}80^{\circ}\text{E}$, $10\text{--}20^{\circ}\text{N}$).

ment in the southwest BOB. This is the line where the first monsoon current advanced into the BOB on 6 June 1995. Thereafter the jet appears to have recognized gradually and extended to southern AS and coincided with the official day of onset on 10 June in Kerala. Figure 2 *d-f* shows the LLJ during the active phase of monsoon (i.e. 10 July, 22 July and 30 August respectively). During these dates the axes of the jet penetrated the west coast of India. India Meteorological Department has reported two break monsoon incidents in this year, on 4–5 July and 12–15 August. It has been reported in several studies that the LLJ is split into two prior to the break monsoon^{7,9}. To verify the above-mentioned phenomenon of splitting, we have plotted the LLJ for the dates 2 July (Figure 2 *g*), 7 and 8 August (Figure 2 *h* and *i*) 1995, followed by plots showing the break (Figure 2 *j-l*). Figure 2 *g* shows the splitting of the LLJ on 2 July. After two days, i.e. on 4 July, the break monsoon can be seen clearly, since there is no LLJ present on the land-mass of the Indian subcontinent; the northern branch of the jet has disappeared and

the southern branch is now passing from the south of the Indian subcontinent. This type of jet split leads to the break conditions. Similarly, on 7 and 8 August (Figure 2 *h* and *i*), one can see the splitting of the jet. Subsequently, on 10 and 11 August (Figure 2 *k* and *l*) there is a break.

Figure 3 shows the time series distribution of the surface meteorological parameters (zonal wind, meridional wind, barometric pressure, air temperature, SST, relative humidity (RH), mixed layer depth at the WHOI buoy (15.5°N , 61.5°E) and AZW) over the AS area ($45\text{--}80^{\circ}\text{E}$, $10\text{--}20^{\circ}\text{N}$) for the period from 1 May to 31 September 1995. Figure 3 *a* shows the time series distribution of the zonal wind (westerly U^+ , easterly U^-) and the meridional wind (southerly V^+ and northerly V^-). The more striking feature is that there exists an organized sudden west to southwesterly flow between 10 and 22 May, with a peak wind speed ($U = 8\text{ m/s}$, $V = 3\text{ m/s}$) on 15 May. This peak wind speed is found to have coincided with the strong surface winds on 15 May, following the depression in the north BOB (Figure 5). Thereafter, the wind returns to its

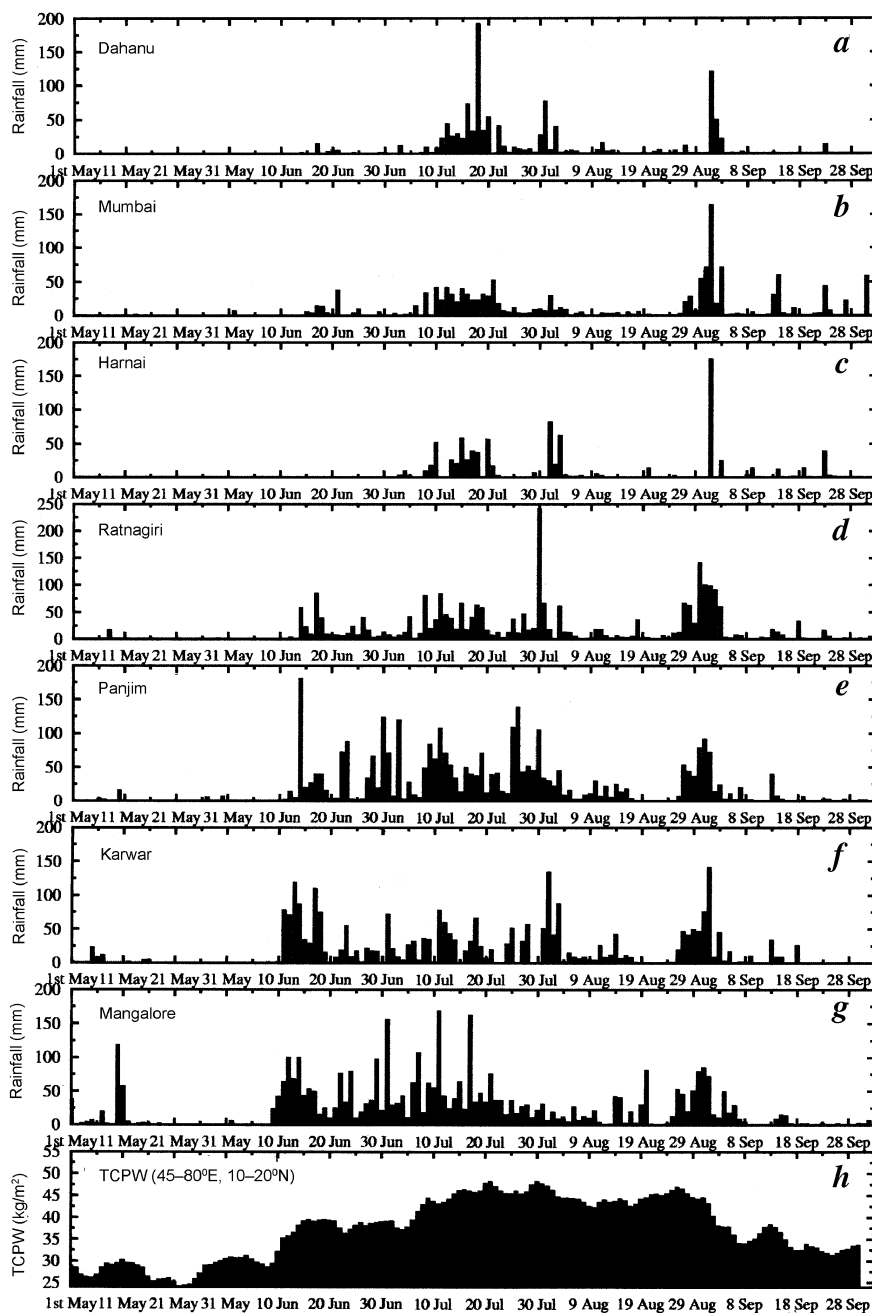


Figure 4. Time series rainfall distribution at selected stations along the west coast (*a–g*), and total column precipitable water (TCPW; *h*) over the area (45–80°E, 10–20°N).

former position (i.e. northeasterly) during 22–31 May. From 1 June onwards the wind becomes westerly to southwesterly and continues to stay at the same position till the end of the monsoon season (June–September). However, the absolute values of the wind speed appeared to have changed from time to time during the above period. The zonal wind attained maximum value of 12 m/s around 15 July, whereas the meridional wind attained a maximum value 9 m/sec around 21 July. There is a progressive decrease in the wind field during August and September. Figure 3 *c* shows the time series barometric

pressure and RH distribution at the WHOI buoy point. It is striking to note that the surface pressure shows high values ≥ 1008 hPa in the month of May and September, while it has shown low values 1001–1008 hPa during the remaining period. The lowest value of 999 hPa has been observed on 10 and 11 July (the corresponding zonal and meridional winds were found maximum). In May, the pressure fluctuations have a great bearing on the wind field. When the pressure is in the peak phase (i.e. ≥ 1008 hPa), the winds exhibit a northeasterly flow at the beginning and end of the month. When the pressure dips to a mini

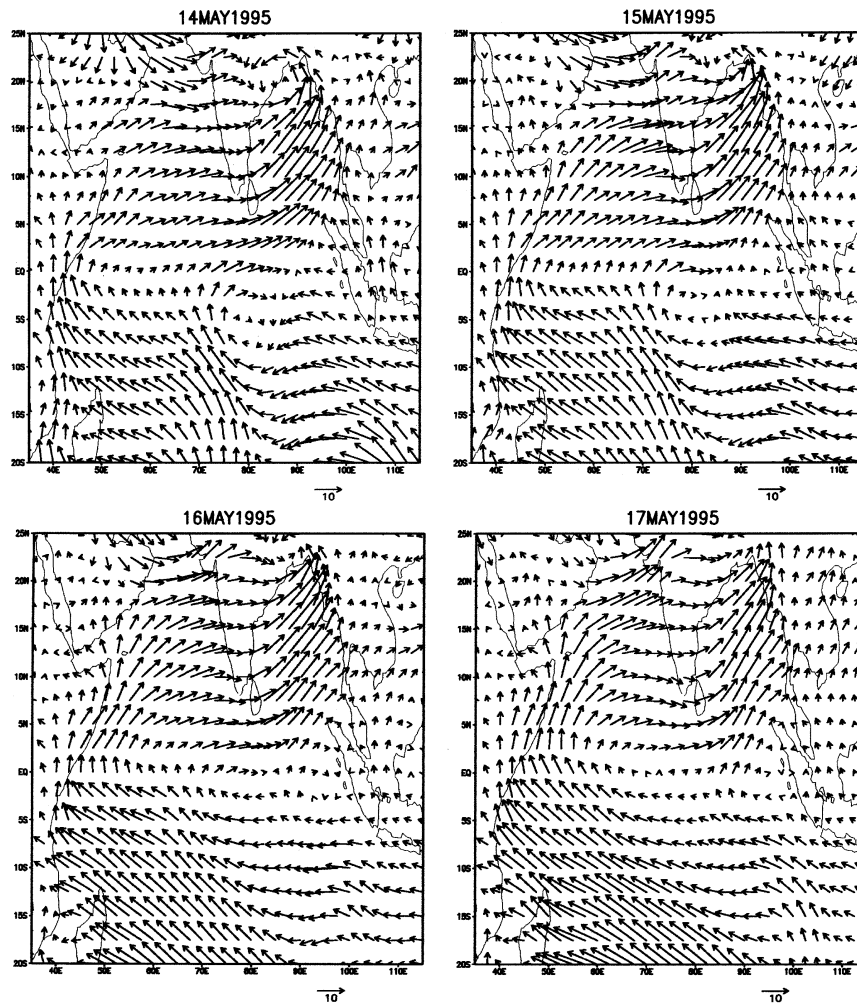


Figure 5. Surface wind pattern during 'bogus' onset.

mum of 1005–1006 hPa, the winds appear to have changed direction from northeasterly to southwesterly between 10 and 20 May, with the lowest pressure value (1005 hPa) coinciding with the higher wind speed on 15 May (see Figure 5). In general, the pressure tends to decrease from 1 May to 15 July and increases from 10 July to 31 September. The RH distribution starts building up to 85% by mid-May and reduces to 65% by the end of May. It starts picking up from 1 June onwards and attains peak values of 90–95% in July and August. Figure 3 *b* shows the time series distribution of SST and air temperature (AT). AT attains a high value of 30°C in the first week of June and a low value (around 26°C) in the first week of August, it again increases to 27°C in September. SST shows a similar trend. It attains a high value of 30.75°C on 31 May, then decreases to a low value of 25.5°C in the first week of August and increases to 28°C in September. The sea water appears to have warmed up rapidly than the air over this region during August and September. However, during May SST is rather uniform with a value of 29.5°C, while AT shows fluctuations but is around 29°C.

MLD (Figure 3 *d*) shows a low value (less than 20 m) in the first and last week of May, while it shows a high value of 30–35 m in the second and third week of May. During June to September it shows the peak, one on 15 July (70 m) and the second on 5 September (50 m), while the lowest value of around 10 m is observed in the first week of May. Figure 3 *d* also shows the time series distribution of daily area AZW speed (45–80°E, 10–20°N) at the sea surface (in the AS), for the period from 1 May to 31 September. The WHOI buoy and the stations along the west coast of India come under this area. The prime reason for considering the average wind speed is to understand whether there is any relevant relationship with the changes in the wind field over the area and at WHOI buoy with the rainfall along the west coast. It is observed from Figure 3 *a* and *d* that both the local and area mean zonal winds appear to have exhibited similar fluctuations during all the months. However, there is a small difference in the magnitude. AZWs are always lower than the local winds at the WHOI buoy. AZWs vary from 1 m/s to the highest value in the second week of July. It is inter-

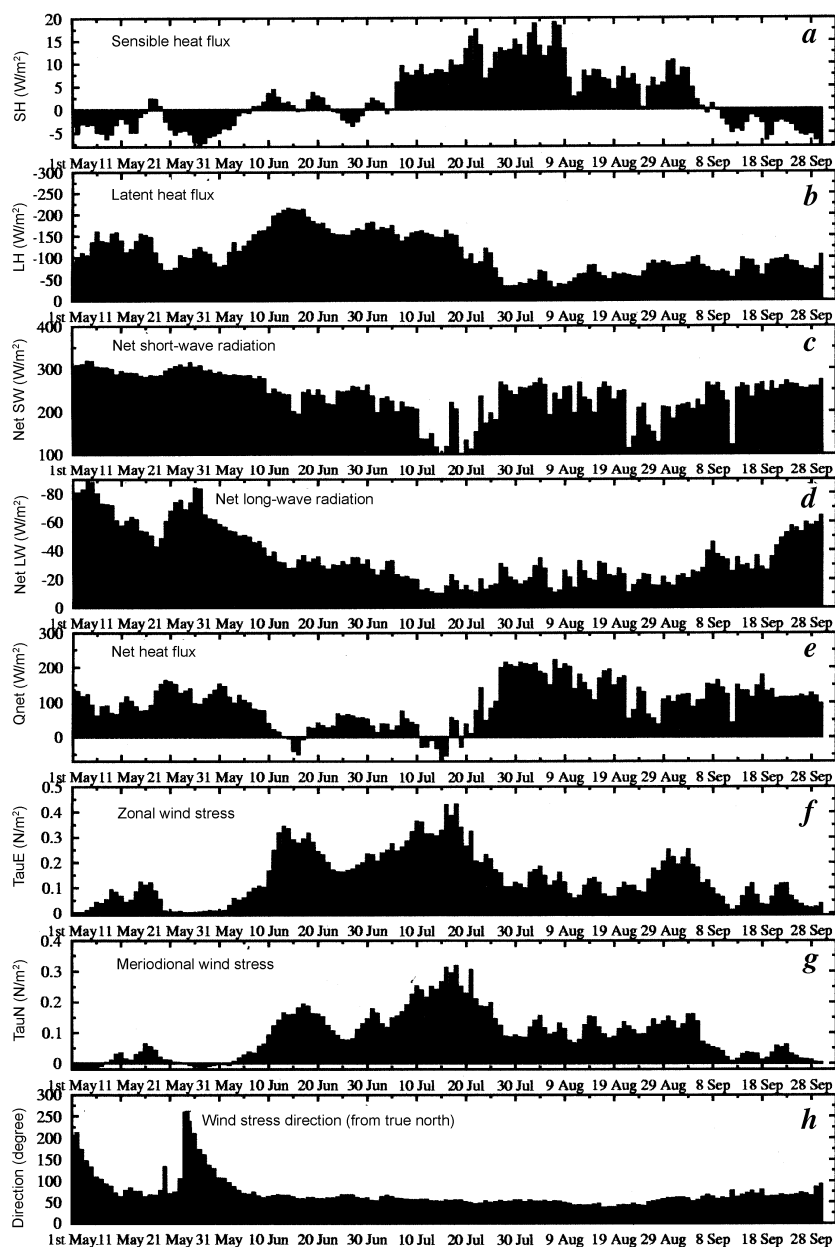


Figure 6. Fluxes of (a) sensible heat, (b) latent heat, (c) net short wave, (d) net long wave and (e) net heat flux with wind stress component (f, g) direction at buoy location (h) (15.5°N, 61.5°E).

esting to note that during 9–18 May the AZW shows a high value of nearly 5 m/s, with a low (1 m/s) on either side. This indicates that wind fields over the AS seem to be sensitive to the depression in the BOB.

Time series distribution of rainfall and TCPW is shown in Figure 4. Rainy days are more at the southern stations of Ratnagiri to Mangalore (Figure 4 d–g), and less in the northern stations of Harnai to Dahanu. Even though rainy days are continuous in the southern stations, there are sporadic spells of high rainfall at an interval of 5 to 10 days in these stations, while there is a large gap of nearly 10–20 days between two heavy spells over the northern stations. It has been noticed that on a few days the rain-

fall data were not available at Harnai and Dahanu. However, the rainfall spells at these two stations are in coherence with rainfall distribution at Mumbai. Figure 4 h shows the distribution of TCPW (in kg/m²) averaged over the domain 45–80°E, 10–20°N. TCPW varies from 28 to 48 kg/m². A low value is observed in May and a high value in July. From 1 May to 10 June, it varies from 28 to 30 kg/m². From 10 June onwards it shows a gradually increasing trend. It remained more or less constant at 48 kg/m² between 10 July and 30 August. The difference between the May maximum and the July maximum of TCPW is 20 kg/m² (48–28 kg/m²). This value gradually increases through a period of about one and half months

Table 1. Monthly and total rainfall (mm) at selected stations in the west coast from May to September

Month → Station ↓	May	June	July	August	September	Total
Dahanu	0 (0)	28 (8)	731.25 (26)	104 (15)	207.75 (10)	1071 (59)
Mumbai	1 (1)	99 (11)	500.5 (29)	262.5 (26)	438.5 (20)	1301.5 (87)
Harnai	0 (0)	0 (0)	372.25 (17)	189.5 (13)	280 (10)	841.75 (40)
Ratnagiri	17.25 (3)	351 (18)	1107.25 (31)	619.5 (28)	357.75 (21)	2452.75 (101)
Panjim	30.25 (6)	743 (20)	1528 (31)	562.25 (24)	202.25 (18)	3065.75 (99)
Karwar	47.25 (7)	768.75 (20)	821.25 (25)	689.75 (26)	297 (12)	2624 (90)
Mangalore	249.5 (14)	1009.25 (24)	1525 (31)	679.5 (28)	244 (17)	3707.25 (114)

Numbers in brackets show the rainy days during the month.

from 1 June to 15 July. Figure 6 *a–h* shows the fluxes of sensible heat, latent heat, net short-wave radiation, net long-wave radiation, net heat flux, zonal wind stress, meridional wind stress and wind stress direction respectively, at the WHOI point. The sensible heat flux at the buoy point is positive from 1 July to 31 August, meandering on either side of the zero value during the rest of the period. It varies from -5 to 20 W/m^2 . Latent heat flux varies from 50 to 200 W/m^2 with a maximum observed between 10 and 20 June and minimum observed around 30 July. The net SW radiation varies between 110 W/m^2 and 300 W/m^2 . Radiational fluxes show similar features, with a maximum in May and September and a minimum in July. The net flux is quite low from 10 June to 20 July and high on either side of this period. Zonal wind stress is strong during the monsoon period. Meridional wind stress also shows similar features in the range 0.1 to 0.4 N/m^2 . The direction of the wind stress is more or less uniform from June to September, around 53° from true north.

Table 1 shows the monthly distribution of total rainfall and total number of days of rainfall occurrence during May to September 1995 along the west coast stations, Dahanu, Mumbai, Harnai, Ratnagiri, Panjim, Karwar and Mangalore. Mangalore received a total rainfall of about 3707 mm in 114 days out of five months (153 days). Panjim received 3065 mm in 99 days. Karwar, Ratnagiri, Mumbai, Dahanu and Harnai received 2624 , 2453 , 1301.5 , 1071 and 842 mm in 90, 101, 87, 59 and 40 days respectively. The northern stations north of Ratnagiri did not receive any rainfall during May except on one occasion at Mumbai. During the monsoon months of June to September, highest rainfall was observed in July at all stations. Panjim received highest rainfall (1528 mm) in July compared to Mangalore (1525 mm). In general, there exists a decreasing trend in rainfall from south to north along the west coast from June to August. In September, the northern stations received high rainfall; Mumbai received 438 mm compared to Mangalore (244 mm) in September.

Discussion

In the foregoing section we have described some salient features of the results obtained on various parameters such as wind field at 850 hPa (Figure 2), surface marine

meteorological observations (Figure 3) and the corresponding fluxes (Figure 6) at the WHOI buoy located close to the climatological LLJ (Findlater jet; Figure 1), and the time series daily rainfall distribution (Figure 4) at selected standard meteorological stations along the west coast of India (Figure 1). In this section we evaluate the salient results. In Figure 4, one can notice the daily rainfall distribution at stations along the west coast of India. Figure 4 also delineates the TCPW over the central AS. The main reason for considering the TCPW over the AS is that the moisture from evaporation in the AS is observed to have provided the water source for the west coast rainfall in particular and Indian rainfall in general^{7,8,10,21,22}. From Figure 4 *g* it can be seen that Mangalore received rainfall from 1 May onwards till the end of September. On 1 May Mangalore received 37 mm of rainfall. The next highest spell of rainfall at this station occurred during 7 to 12 May 1995. During the same period Ratnagiri, Panjim and Karwar (Figure 4 *d–f*) also received good rainfall. After 12 May, there was a lull in the rainfall at all the above stations, except a small amount of rainfall ($2–3 \text{ mm}$) on some occasions. However, the next big spell of heavy rainfall commenced from 9 June in Panjim, Karwar and Mangalore (Figure 4 *e–g*). Dahanu, Mumbai and Ratnagiri (Figure 4 *a, b* and *d*) have received rainfall after 15 June. There are several occasions of heavy to very heavy rain spells at Mangalore, Karwar, Panjim and Ratnagiri from 10 June to 10 September. All these stations received these spells more or less at the same time or a lag of one or two days. But the northern stations of Dahanu, Harnai and Mumbai received only three heavy spells occurring at an interval of 15 to 20 days. Comparing Figure 4 *a–g* with the Figure 4 *h*, one can clearly understand the behaviour of rainfall along the west coast and build-up of moisture content over Arabia.

It can be seen from TCPW observations (Figure 4 *h*) that this parameter appears to have exhibited a rise and fall in the value approximately at an interval of 5–10 days during the period of observation. During the period from 1 May to 10 June, TCPW shows three ridges and three troughs. The lowest value is 25 kg/m^2 between 22 and 24 May. Peaks are observed on 1 May, 10 May and 4 June and the values are 28 , 30 and 32 kg/m^2 respectively. After 4 June, TCPW increases rapidly till August, with a small

dip on 8 June. Whenever there is an increase in TCPW over the AS, there is a corresponding rainfall event at Mangalore, Karwar and Panjim during period from 1 May to 5 June. Following 5 June, there appears to be a fall in TCPW between 6 and 8 June and thereafter a continuous rise steeply from 9 June onwards. This is the time when the northern limit of the monsoon advanced northward and the first spell of the monsoon rainfall occurred over Mangalore on 9 June, Karwar on 11 June, Panjim on 12 June and Ratnagiri on 14 June. The northern stations did not receive monsoon rains. After 10 June onwards when TCPW begins to increase over the AS, all the west coast stations started receiving moderate to heavy rainfall throughout the monsoon months. However, there are some heavy spells of rainfall epochs at all stations during 10–22 July, 30 July–2 August and 25 August–6 September. During these epochs TCPW appears to be at its maximum value ($\geq 50 \text{ kg/m}^2$). Comparison of the above spell with the 850 hPa LLJ core and orientation of its axis shows coherence in the west coast rainfall, TCPW build-up in the AS and the perpendicular incidence of the axis of the LLJ to the west coast of India during 10–13 June (example, Figure 2*b* and *c*), 10–20 July (Figure 2*d* and *e*), 30 July–2 August and 25 August–6 September (Figure 2*f*). The positive U and V components of the wind field at WHOI buoy location (Figure 3*a* and *b*), and the AZW are observed to be quite high during the above period, which coincide with the strong LLJ and the corresponding rainfall along the coast. This type of strong wind at the surface in the AS appears to have picked up moisture from the ocean, injected it into the lower atmosphere in the open ocean and carried the moisture along the jet core to deliver rainfall along the west coast of India and inland, perhaps, during the above period of observation⁵. The surface pressure (Figure 3*c*) appears to be lower during the above period of heavy rainfall along the west coast. During the period of little or no rainfall along the west coast, the LLJ appears to have either split⁷ (2 July, 7 and 8 August; Figure 2*g–i*) or weakened (4 July, 10 and 12 August; Figure 2*j–l*). During the above-mentioned days, winds at the WHOI buoy are also weaker and hence the corresponding TCPW content.

It is important to note here that the rainfall occurred over the south stations of Mangalore, Karwar and Panjim during the dry month of May. This rainfall appears to have occurred in association with some low-pressure (deep depressions) disturbances in the BOB during 5–6, 8–10 and 14–17 May. All the above systems are reported²⁰ to be deep depressions formed off the Coromandal coast of India. During the above period (5 to 17 May), the wind field (U^+ and V^+) appears to have increased rapidly (attains a maximum value 8 and 3 m/s respectively, on 15 May) and the corresponding TCPW also showed a similar trend. While examining year-long time series data at WHOI buoy, Weller *et al.*¹¹ reported that at the time of the SW monsoon the wind speed rose initially in early May, then be-

came light, before rising again in early June (Figure 3*a* and *b*). This is in agreement with the results of Fieux and Stommel²³ during the years they characterized as having multiple onset. Recently Flatau *et al.*²⁴ studied the dynamics of double monsoon onset (multiple onset or bogus onset) over India. As reported in the foregoing discussion, we have seen that the winds attain maximum speed on 15 May and 9 June at the WHOI buoy. These two dates correspond to the double/multiple onsets in 1995. Since they match well with the Fieux–Stommel²³ hypothesis, Flatau *et al.*²⁴ have tried to understand the plausible reasons for the occurrence of the above double onset. In fact, they have named the first onset as ‘bogus’ onset over the AS. Further, they have briefly summarized the dynamical conceptual model as follows. In early May, Madden Julian oscillation develops in the equatorial IO. Warm SST anomaly appears to be present in the BOB and in the western Pacific. In mid-May the equatorial convection splits, with one branch propagating into the western Pacific (warm SST) and another branch moving into the BOB (warm SST), thus initializing ‘bogus’ monsoon onset. The descending branch of the Walker cell, related to the convection in western Pacific, and the Hadley cell related to ‘bogus’ onset, suppresses the equatorial convection. In late May and early June, the BOB convection dies, SSTs become low in the Bay because of the ‘bogus’ onset of the monsoon, but hot and dry conditions dominate over the land. The real onset gets delayed because of the previously established conditions. The May rainfall along the west coast is observed to have occurred due to the three systems in the BOB, whereas rainfall after 9 June is purely due to monsoon circulation and the associated strong LLJ.

The convection in BOB appears to have initiated the development of the fairly strong southwesterly flow over the BOB and fairly westerly winds over the AS (14–17 May; WHOI; Figure 3*a*) and 14 May²⁴, Flatau *et al.*²⁴ have considered SST, wind velocity (U^+ and V^+) and specific humidity at WHOI buoy to show the time of bogus onset. But they have removed the perturbations with a timescale longer than 90 days and shorter than five days. They have also shown similar features found in the present study.

In order to understand the plausible reason for the occurrence of strong westerly winds at WHOI, the 850 hPa circulation charts for the period from 14 to 17 May (Figure 5) have been analysed. A core of LLJ-like wind field is seen over the BOB, extending from north India, north AS to Arabia. The LLJ during the above period intensifies in the wake of a depression that is formed over the north BOB²⁵. The influence of this system on the 850 hPa wind field over the AS as seen in Figure 5, as well as on the surface wind field over the WHOI buoy, has been observed at the time of recording. This 850 hPa wind field further shows that the winds in the AS south of the WHOI buoy are completely westerly and those to the

north of the buoy are northwesterly, keeping low variable wind near the buoy. Mangalore received good rainfall due to the prevailing strong westerly over land, while absence of rainfall over the northern stations along the west coast during the same period may be due to the prevailing dry northwesterly winds coming from the relatively cold AS surface during 14–17 May. While developing a conceptual/dynamical model for identifying the plausible reasons for the multiple onset over the Indian seas (AS and BOB), Flatau *et al.*²⁴ have concluded that the intra-seasonal oscillation in convection at the equator, 60°E and its eastward propagation along the equator up to 90°E, touch warm SST resulting in monsoon-like meteorological conditions.

This study concludes that LLJ plays an important role in determining the rainfall variability over the west coast of India. It is seen that during the active phase of monsoon, the LLJ is elongated in west-east direction over the Indian peninsula. Prior to the break, splitting of the LLJ takes place due to forced flow from the north; the northern branch of the LLJ disappears and southern branch passes through the south of the Indian subcontinent taking all the moisture towards the equator. This is known as break in monsoon, which was experienced during 4–5 July and 12–15 August 1995. LLJ is a good indicator of active and break phases of monsoon over the country. Keeping a constant watch on LLJ, one can get the information regarding break and active phases of the monsoon well ahead of time. Air–sea interaction and flux study on the buoy location prove that the SW monsoon 1995 had strong winds, cloudy skies and moist air and was accompanied by sustained oceanic heat gain with strong warming.

1. Findlater, J., A major low-level current near the Indian Ocean during the northern summer. *Q. J. R. Meteorol. Soc.*, 1969, **95**, 362–380.
2. Bunker, A. F., Interaction of the summer monsoon air with the Arabian Sea. Proc. Symp. on Met. Results of the IIOE, Mumbai, 1965, p. 3.
3. Joseph, P. V. and Raman, P. L., Existence of low-level westerly jet streams over peninsular India. *Indian J. Meteorol. Geophys.*, 1966, **17**, 407–410.
4. Findlater, J., Mean monthly air flow at low levels over the western Indian Ocean. *Geophysics Memoirs*, Her Majesty's Office, London, 1971, **115**, pp. 1–53.
5. Krishnamurti, T. N. (ed.), *Monsoon Dynamics, Contributions to Current Research in Geophysics*, Birkhauser Verlag, 1978, pp. 1087–1529.
6. Stommel, H. and Fioux, M., *Oceanographic Atlases – A Guide to their Geographic Coverage and Contents*, Woods Hole Press, Massachusetts, USA, 1978.
7. Swapna, P. and Ramesh Kumar, M. R., Role of low-level flow on the summer monsoon rainfall over the Indian subcontinent during two contrasting monsoon years. *J. Indian Geophys. Union*, 2002, **6**, 123–137.
8. Vinayachandran, P. N., Sadhuram, Y. and Ramesh Babu, V., Latent and sensible heat fluxes under active and weak phase of the summer monsoon of 1986. *Proc. Indian Acad. Sci.*, 1989, **98**, 213–222.
9. Sijikumar, S., Sathiyamoorthy, V., Anu, S., Prince, K. X., Sajith, V. and Joseph, P. V., Does the low-level jet stream split into two branches over the Arabian Sea? *Tropmet 2000: Ocean and Atmosphere*, 2000, pp. 167–172.
10. Ramesh Kumar, M. R., Sheno, S. S. C. and Schluessel, P., On the role of the cross equatorial flow on summer monsoon rainfall over India using NCEP/NCAR reanalysis data. *Meteorol. Atmos. Phys.*, 1999, **70**, 201–213.
11. Weller, R. A., Baumgartner, M. F., Josey, S. A., Fischer, A. S. and Kindle, J. C., Atmospheric forcing in the Arabian Sea during 1994–95 observations and comparisons with climatology models. *Deep Sea Res. II*, 1998, **45**, 1961–1999.
12. Indian Daily Weather Report, IMD Pune.
13. Kalney, E. *et al.*, The NCEP/NCAR 40-year reanalysis project. *Bull. Am. Meteorol. Soc.*, 1996, **77**, 437–471.
14. Seetaramayya, P., Pattanaik, T. and Gnanaseelan, C., On the air–sea interactions in the central Arabian Sea at 15.5°N, 61.5°E. Proc. of the National Symp. on Prediction of Meteorological Events of Mathematical Approach, BIT Mesra 25–26 March 2003, in press.
15. Gnanaseelan, C., Mishra, A. K., Thompson, B. and Salvekar, P. S., Thermodynamics and dynamics of the upper ocean mixed layer in the central and eastern Arabian Sea. IITM Research Report No. RR-098, August 2003, pp. 1–37.
16. Fairall, C. W., Bradley, E. F., Rogers, D. P., Edson, J. B. and Young, G. S., Bulk parameterization of air–sea fluxes for tropical ocean–global atmosphere coupled ocean atmosphere response experiment. *J. Geophys. Res.*, 1996, **101**, 3747–3764.
17. Payne, R. E., Albedo of the sea surface. *J. Atmos. Sci.*, 1972, **29**, 959–970.
18. Ananthakrishnan, R., Pathan, J. M. and Aralikatti, S. S., The onset phase of the southwest monsoon. *Curr. Sci.*, 1983, **52**, 155–164.
19. Ananthakrishnan, R. and Soman, M. K., The onset of the southwest monsoon over Kerala 1901–80. *J. Climatol.*, 1988, **8**, 283–296.
20. Sikka, D. R., Paul, D. K., Deshpande, V. R., Majumdar, V. R. and Puranik, P. V., Subseasonal scale fluctuations of the ITCZ over the Indo-Pacific region during the summer monsoon season: Part I: Features over the Indian region. *Proc. Indian Acad. Sci. (Earth Planet. Sci.)*, 1986, **95**, 47–73.
21. Pearce, R. P. and Mohanty, U. C., Onset of the Asian summer monsoon 1979–82. *J. Atmos. Sci.*, 1984, **41**, 1620–1639.
22. Sadhuram, Y., Ramesh Babu, V., Gopalkrishnan, V. V. and Sarma, M. S. S., Association between premonsoonal SST anomaly field in the eastern Arabian Sea and subsequent monsoon rainfall over the west coast of India. *Indian J. Mar. Sci.*, 1991, **20**, 106–109.
23. Fioux, M. and Stommel, H., Onset of the southwest monsoon over the Arabian Sea from marine reports of surface winds: structure and variability. *Mon. Weather Rev.*, 1977, **105**, 231–236.
24. Flatau, M. K., Flatau, P. J. and Rudnick, D., The dynamics of double monsoon onsets. *J. Climate*, 2001, **14**, 4130–4146.
25. Roy Bhowmik, S. K. and Misra, P. K., Some structural characteristics of pre-monsoon depression in the Bay of Bengal. *Mausam*, 1999, **50**, 19–24.

ACKNOWLEDGEMENTS. We thank the Director, IITM and the Head, Theoretical Studies Division, IITM for providing the required infrastructure. We also thank R. A. Weller, T. D. Dickey and J. Marra for providing meteorological and oceanographic data at WHOI point. Financial assistance was provided by Department of Science and Technology, Government of India. Suggestions made by the anonymous referee have helped to improve the manuscript.

Received 2 January 2004; revised accepted 24 March 2004